

Dalton Transactions

Accepted Manuscript

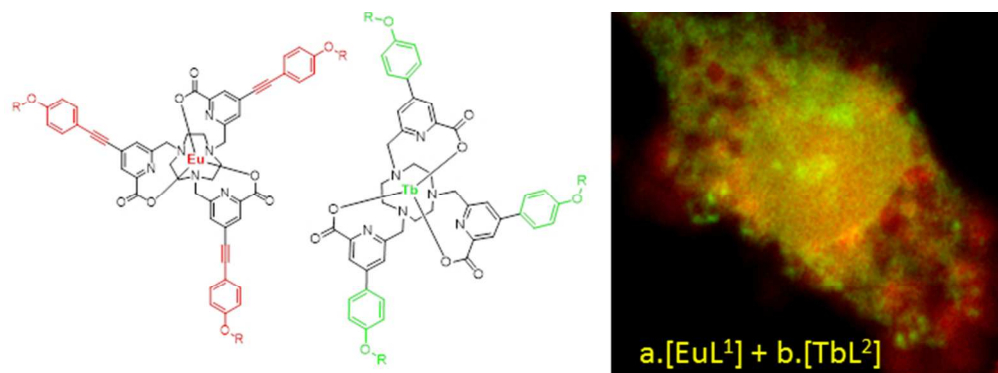


This is an *Accepted Manuscript*, which has been through the Royal Society of Chemistry peer review process and has been accepted for publication.

Accepted Manuscripts are published online shortly after acceptance, before technical editing, formatting and proof reading. Using this free service, authors can make their results available to the community, in citable form, before we publish the edited article. We will replace this *Accepted Manuscript* with the edited and formatted *Advance Article* as soon as it is available.

You can find more information about *Accepted Manuscripts* in the [Information for Authors](#).

Please note that technical editing may introduce minor changes to the text and/or graphics, which may alter content. The journal's standard [Terms & Conditions](#) and the [Ethical guidelines](#) still apply. In no event shall the Royal Society of Chemistry be held responsible for any errors or omissions in this *Accepted Manuscript* or any consequences arising from the use of any information it contains.





Two-photon multiplexing bio-imaging using a combination of Eu- and Tb-bioprobes.

Virginie Placide,^a Anh Thy Bui,^a Alexei Grichine,^{b,c} Alain, Duperray,^{b,c} Delphine Pitrat,^a Chantal Andraud,^{a*} and Olivier Maury^{a*}

During the course of our researches aiming to combine the unique photophysical properties of lanthanide complexes and the intrinsic advantage of a nonlinear two-photon excitation, we described the proof-of-concept of biphotonic multiplexing bio-imaging experiment. To that end, a new Tb-luminescent bioprobe [TbL²] was designed using the TACN-trispicolate platform. The biphotonic imaging of T24 fixed cells stained either with [TbL²] or with the already described [EuL¹] complexes is reported. Finally the biphotonic multiplexing experiment was achieved using the combination of both probes using the spectral mode of the two-photon microscope.

Introduction

For about one decade, the tremendous development of biphotonic microscopy for bio-imaging applications triggered the emergence of a new field of research aiming at combining the intrinsic advantages of two-photon excitation and the unique photophysical properties of lanthanide ions.¹ Two-photon (2P) excitation allows a 3D resolution, with an excitation in the near-infrared spectral range and results in reduced photo-bleaching and photo-damage and numerous organic dyes featuring optimized two-photon brightness have been reported for this application.² On the other hand, f-block elements are well known for their sharp emission bands characteristic of each element with long lifetime enabling time-resolved and multiplexing imaging.³ The combination of these properties in a new generation of biphotonic lanthanide luminescent bio-probes (LLB) should strongly enhance the potentialities of biphotonic microscopy. Following initial proof-of-concept of sensitisation of lanthanides luminescence by two-photon antenna effect,⁴ in 2008 were independently reported the first biphotonic bio-imaging experiments using Eu(III) or Tb(III) probes.⁵ After these benchmark experiments many other Eu, Tb complexes were used as 2P-LLB,⁶ and their scope was extended to Yb(III) luminescent compounds emitting in the near infrared spectral range⁷ enabling thick tissues 3D bio-imaging⁸ towards the biphotonic detection of ultrabright single nano-objects.⁹ Very recently, we demonstrated the feasibility of ms-lifetime imaging including 2P-FRET experiment (TSLIM) and we extended the time-resolved imaging (PSLIM) with a two photon excitation using a conventional microscope.¹⁰ Herein we reported the proof-of-concept of 2P-multiplexing experiment using a combination of Tb(III) and Eu(III) 2P-LLB.

Multiplexing experiment consists in recording simultaneously the luminescence of several lanthanide bio-markers using the same excitation and in reconstructing *in silico* the image related to each marker thanks to the spectral sharpness of the *f*-element transitions. This technique has been widely used for multicolour 1P-bioimaging or for high throughput multi-labels fluoroimmunoassay¹¹ but was never combined with a two-photon excitation. To that end, we designed an original 2P-terbium(III) bioprobe, [TbL²] based on the very stable tris-picolinate-triazacyclononane platform using the same approach successfully employed for ytterbium(III)⁸ and more recently for europium(III) derivatives (including [EuL¹], chart 1).¹² The π -conjugated charge transfer (CT) antenna in [TbL²] was shorted compare to that of [EuL¹] in order to sensitise the higher energy ⁵D₄ terbium emitting state. This article described the synthesis of [TbL²] and compared its photophysical properties with those of [EuL¹]. The biphotonic cells imaging was performed with either the terbium or europium markers alone or using the combination of both probes.

PREPRINT

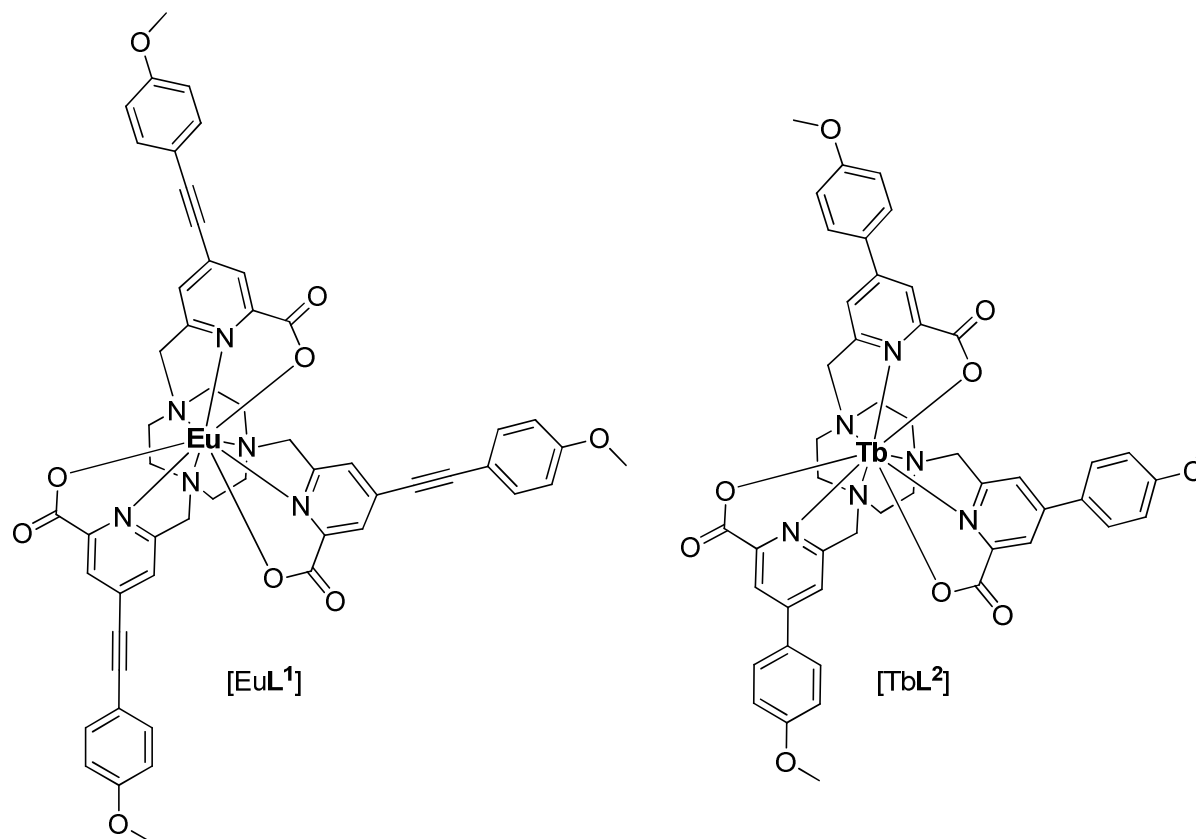
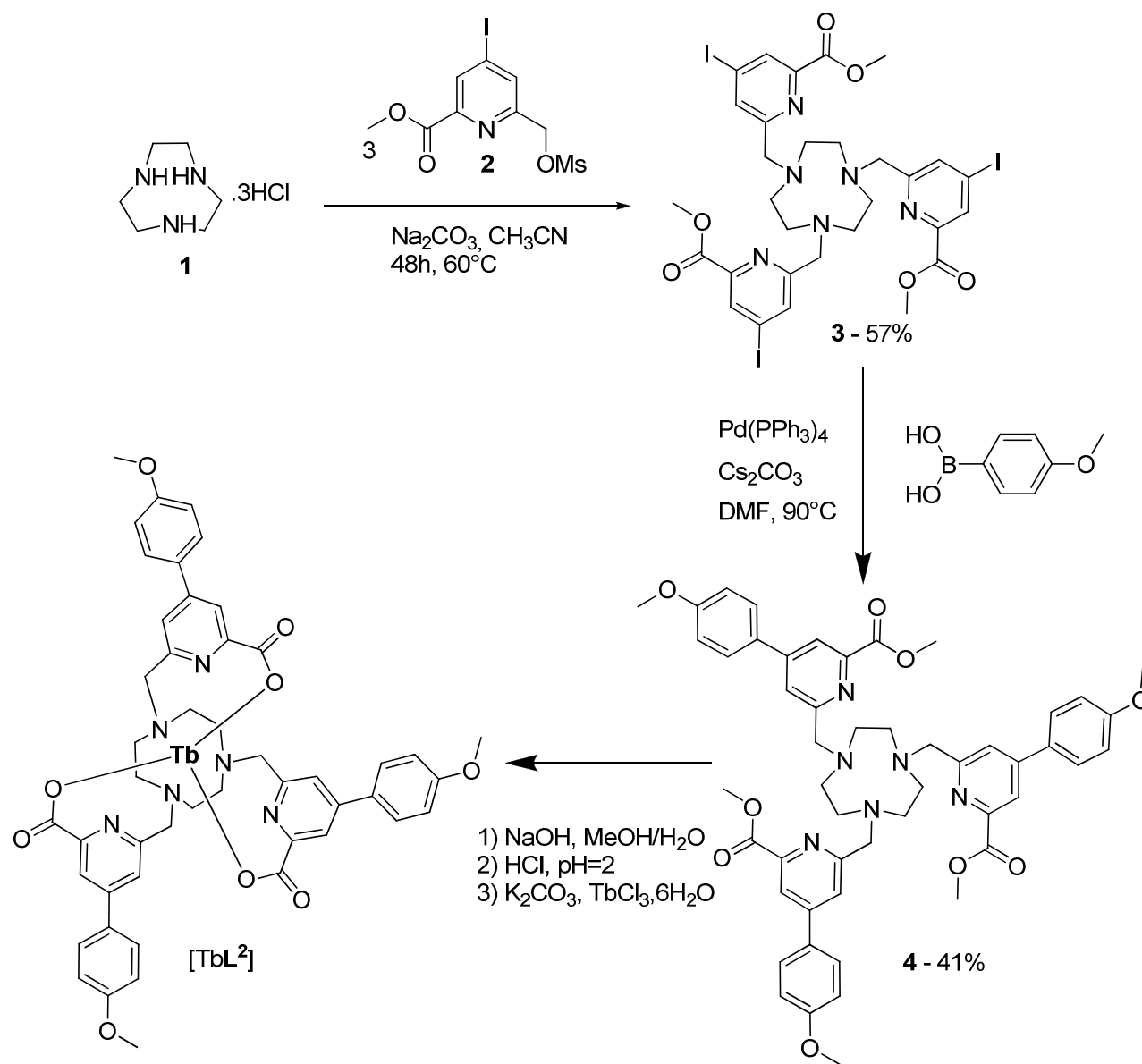


Chart 1. Structure of the 2P-bioprobes, [EuL¹] and [TbL²].

Results and discussion

A Synthesis

The preparation and characterisation of [EuL¹] has already been described.¹² The synthesis of ligand **4** precursor of [TbL²] was achieved using the convergent pathway described in scheme 1.¹³ In a first step the iodinated tris-picolinate TACN platform (**3**) was prepared by alkylation of 1,3,7-triazacyclononane-trishydrochloride (**1**) with the mesylated compound **2** in dry CH₃CN. This platform prepared on large scale is becoming a key synthon for the preparation of a large variety of functionalised ligands using cross-coupling reactions.¹⁴ In the present case, **4** was prepared with a 40% yield using the Suzuki-Miyaura coupling of anisole boronic acid in DMF at 90°C with Pd(Ph₃)₄ as catalyst and Cs₂CO₃ as a base. The terbium complex was prepared using similar procedure than that used for its europium analogous: (i) a saponification of the ester moieties of **4** by sodium hydroxide followed (ii) by the acidification of the reaction media with aqueous hydrochloric acid and (iii) a final reaction with a terbium salt in the presence of carbonate. The complex was purified by several titrations and precipitations, isolated as a white microcrystalline powder and characterized by HPLC and high-resolution mass spectrometry.

Scheme 1. Synthesis of the [TbL²].

B Spectroscopic properties

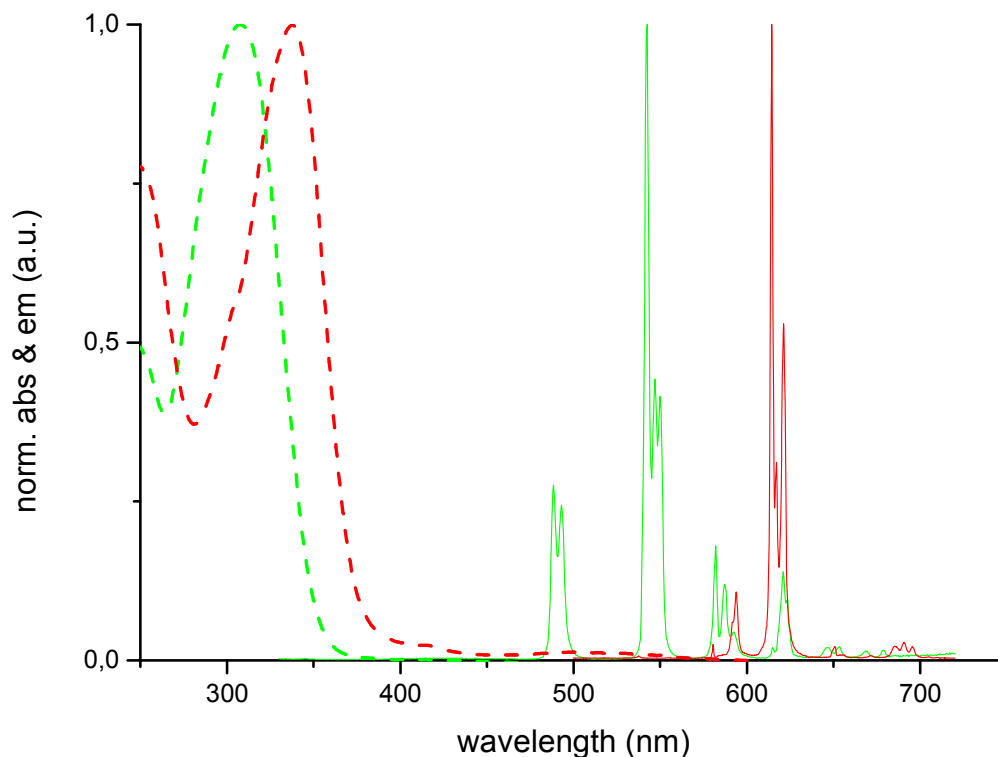


Figure 1. Normalised absorption (dashed line) and emission (full line) of $[\text{EuL}^1]$ in red and $[\text{TbL}^2]$ in green at room temperature in MeOH solution.

The photophysical properties of both compounds have been studied in diluted methanol solution, absorption and emission spectra are reported in the figure 1. The $[\text{EuL}^1]$ complex is one of the brightest europium derivatives with a strong absorption at 338 nm ($\epsilon = 58000 \text{ L.Mol}^{-1}.\text{cm}^{-1}$), a high quantum yield of 48% ($\tau = 0.95 \text{ ms}$) and an acceptable two-photon cross-section of 49 GM at 700 nm.¹² The $[\text{TbL}^2]$ complex exhibited a less conjugated antenna composed of a simple bi-aryl conjugated chain substituted by a weak electro-donating methoxy fragment. As a result the charge transfer absorption band (308 nm, $\epsilon = 33000 \text{ L.Mol}^{-1}.\text{cm}^{-1}$) is blue shifted by 30 nm compared to the europium analogous. This antenna is suitable to sensitize efficiently the Tb(III) luminescence as illustrated by the absence of any residual ligand centred emission. The quantum yield and lifetime remain rather modest ($\Phi = 12\%$, $\tau = 0.24 \text{ ms}$) compared to related non-substituted complex.¹⁵ Although back energy transfer cannot be completely excluded, these low values can be explained by the free aryl-aryl rotation, increasing non-radiative relaxation pathways. This hypothesis was corroborated by the significant exaltation of the lifetime to 0.63 ms in glycerol, a more viscous solvent where this rotation is more difficult. The two-photon cross-section of this derivative was not precisely measured since it lies mainly out of the Ti:sapphire laser spectral range (700-1050 nm) and only the red-tail can be qualitatively observed. As illustrated by the figure 1, it is worth noting that these two $[\text{EuL}^1]$ and $[\text{TbL}^2]$ compounds present very distinct transitions making them suitable for a multiplexing experiment. In particular the $^5\text{D}_4 \rightarrow ^7\text{F}_6$ and $^5\text{D}_4 \rightarrow ^7\text{F}_5$ transitions at 490 and 543 nm respectively are perfectly isolated from the signals of europium and are a clear signature of the presence of the terbium derivative. On the other hand, the hypersensitive $^5\text{D}_0 \rightarrow ^7\text{F}_2$ at 615 nm is representative for $[\text{EuL}^1]$ in spite of an overlap with the weak $^5\text{D}_4 \rightarrow ^7\text{F}_3$ transition of $[\text{TbL}^2]$.

C. Two-photon microscopy imaging.

These two complexes are not well soluble in water consequently the staining experiments were carried out by addition of a small amount (10-100 μL) of a concentrated DMSO solution (10^{-3} - 10^{-4} M) to PBS (1 ml). In a first time, T24 cancer cells fixed with paraformaldehyde, were stained either with $[\text{EuL}^1]$ or $[\text{TbL}^2]$ alone (figure 3). The cell images including *in situ* probes emission spectra were registered under a biphotonic excitation ($\lambda_{\text{ex}} = 720 \text{ nm}$) as described in the experimental section. A single wide

spectral detection channel was used in these cases and no spectral deconvolution was performed. It should thus be noted that the small punctuate structures at the cell periphery may result from the contribution of autofluorescence. The two probes clearly stained the endoplasmic reticulum and the nucleosol with a higher concentration of $[\text{TbL}^2]$ in the nucleoli. The emission spectra of both LLB can be monitored *in cellulo* using the spectral detection mode of the microscope with a resolution of *ca.* 10 nm. In spite of this quite low resolution, the characteristic Eu(III) and Tb(III) signals appear very distinctly. For sake of comparison, cells stained with $[\text{EuL}^1]$ were imaged with a single photon (1P) excitation at 405 nm and the emission spectrum was recorded (figure 2). Whereas cells images look very similar to that recorded with a two-photon excitation at, the emission spectrum exhibits a broad signal centred at 470 nm in addition to the Eu(III) sharp bands. This wide-band signal, due to the contribution of cellular autofluorescence is reduced under 2P excitation and the 2P-images present consequently a higher signal-over-noise ratio.

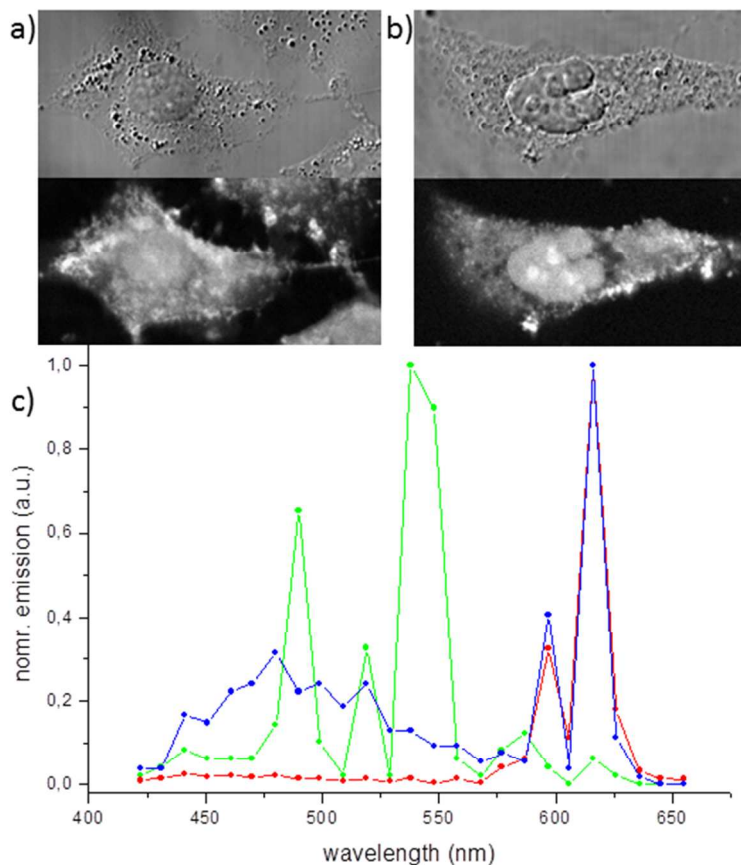


Figure 2. Images of T24 cells after paraformaldehyde fixation and staining with $[\text{EuL}^1]$ (a) or $[\text{TbL}^2]$ (b). Images were taken in transmitted light differential interference contrast (DIC, up) and two-photon laser scanning ($\lambda_{\text{ex}} = 720$ nm, down). c) *In cellulo* emission spectra of $[\text{EuL}^1]$ (red) and $[\text{TbL}^2]$ (green) under 2P-720 nm excitation and of $[\text{EuL}^1]$ under 1P-405nm excitation (blue).

The multiplexed imaging was then possible due to the distinct spectral signatures of the two lanthanide complexes. Their sharp emission peaks and firm peak-to-peak intensity ratios allowed a quantitative discrimination of the relative contribution of each complex after spectral deconvolution, even if some minor peaks do overlap. It should be stressed here, that the spectral unmixing is possible not only for the dyes of different “colours” but for any combination of lanthanide derivatives with the intermingled emission peaks. In fact, the unmixing acts not only as a tuneable dichroic or band-pass filter, but takes into account the whole spectral shape and may be sensitive to small variations in any part of the spectrum. The limited spectral resolution of a confocal microscope (*ca.* 10 nm) was however sufficient for the faithful discrimination of species and presented the advantage of increasing the number of photons per channel. This feature is especially important in confocal microscopy where the measured volume in each voxel is very small (0.2 fL) and the concentration of the species is variable and may be very low. In the present case, the cells were stained with a mixture of $[\text{EuL}^1]$ and $[\text{TbL}^2]$ and the 2P-images were acquired using the spectral mode of the microscope. The resulting emission spectra (figure 3) is composed of the Tb(III) and Eu(III) transitions and of a weak contribution of cellular auto-fluorescence. The spectral deconvolution (or linear unmixing) procedure allows reconstruction of an image related to each single component (figure 3) after elimination of parasitic auto-fluorescence. It is then possible to normalise and recombine these

PREPRINT

two images affected with a green (Tb) and a red (Eu) colours, respectively. In the reconstructed image, the green and red areas indicate the major presence of $[\text{TbL}^2]$ and $[\text{EuL}^1]$, respectively whereas the yellow areas indicate a mixing of both dyes.

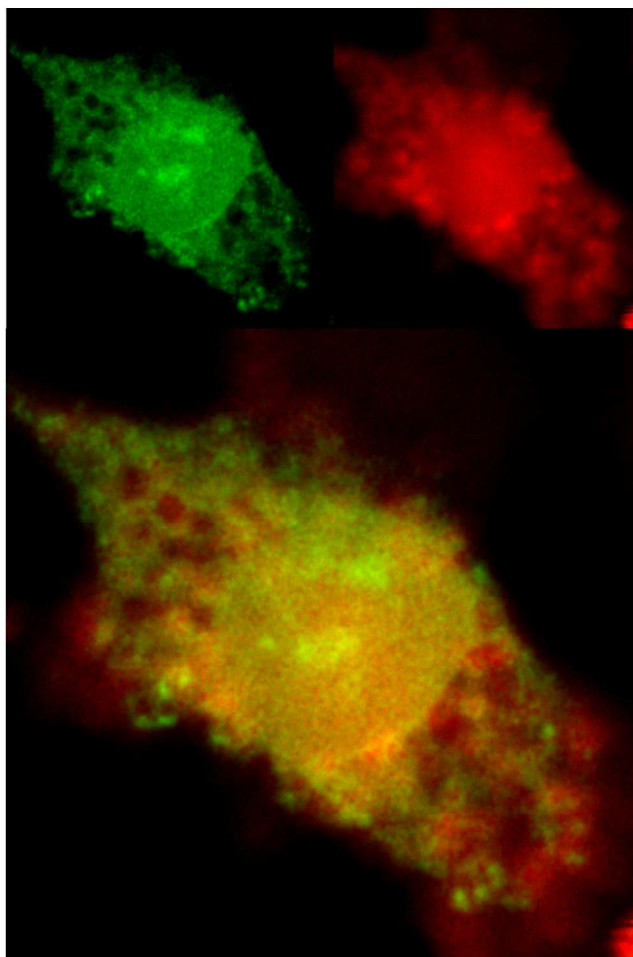
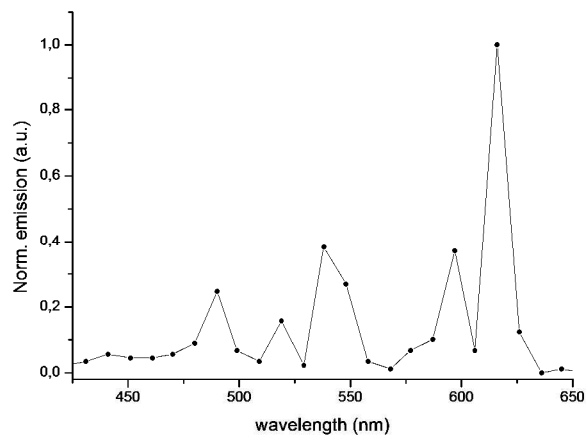


Figure 3. Two-photon multiplexing imaging experiments of fixed T24 cells stained with $[\text{EuL}^1]$ and $[\text{TbL}^2]$. (top) multiplexed emission spectra. (Middle) 2P-images obtained after linear unmixing procedure corresponding to Tb (green) and Eu (red) spectral deconvolution. The contribution of the weak 2P-auto-fluorescence has been previously subtracted. (bottom) reconstructed multiplexed images by normalisation and addition of the two aforementioned images.

Conclusion

In conclusion this article described the synthesis and characterisation of a new [TbL²] 2P-LLB based on the triazacyclononane trispicolinate platform, belonging to the same family as the benchmark [EuL¹] complex. These two derivatives were successfully used as markers for the 2P-scanning microscopy imaging of fixed cells. Finally the multiplexed imaging was possible using a co-staining with the two probes thanks to the distinct spectral signatures of the two lanthanide ions. This type of experiment is classical in linear microscopy but was never achieved under two-photon excitation. Combined with the recently demonstrated long luminescence lifetime imaging (TSLIM) and time gated (PSLIM) 2P-microscopy,¹⁰ it is now possible to fully exploit the unique luminescence properties of lanthanides in biphotonic microscopy and to achieve both spectral and temporal resolution. These combined detections associated with specific functions for the targeting of different cell-compartments would open the way for a high-content multi-parameters multiplexed labelling.

Experimental

General. Starting materials were purchased from Sigma Aldrich®, Acros Organics® or Alfa Aesar® with the best available quality grade and were used without further purification. **2** has been prepared using the procedure described in the literature.¹⁶ NMR spectra (¹H, ¹³C) were recorded at room temperature on a BRUKER® Advance operating at 500.10 MHz and 125.75 MHz for ¹H and ¹³C, respectively. Data are listed in parts per million (ppm) and are reported relative to residual solvent peaks being used as internal standard (¹H (CDCl₃): 7.26 ppm, ¹³C (CDCl₃): 77.2 ppm; ¹H (CD₃OD): 3.31 ppm, ¹³C (CD₃OD): 49.0 ppm). UV-visible spectra were recorded on a Jasco® V-670 spectrophotometer in spectrophotometric grade methanol (ca. 10⁻⁵ or 10⁻⁶ mol L⁻¹). Molar extinction coefficients were determined at least two times. Emission spectra were measured using a Horiba-Jobin-Yvon Fluorolog-3 fluorimeter. The steady-state luminescence was excited by unpolarized light from a 450 W xenon CW lamp and detected at an angle of 90° for diluted solution measurements (10 mm quartz cuvette) by Hamamatsu R928 photomultiplier tube. Spectra were corrected for both the excitation source light intensity variation and the emission spectral response. Phosphorescence lifetimes were obtained by pulsed excitation using a FL-1040 UP Xenon Lamp. Luminescence decay curves were fitted by least-squares analysis using Origin®. Luminescence quantum yields *Q* were measured in diluted water solution with an absorbance lower than 0.1. Here, reference is quinine bisulfate in 1N aqueous sulfuric acid solution (*Q*_r = 0.546). Excitation of reference and sample compounds was performed at the same wavelength. Column chromatography was performed with Acros Organics® (0.035-0.070 mm) silicagel. HPLC was performed on a Agilent Technologies 1260 Infinity apparatus equipped with a Waters XBridge RP-C18 column, (3.5 μm, 4.6 × 100 mm). Experimental condition ammonium formate 0.25M-MeCN (v/v) as eluents: isocratic MeCN (2 min), linear gradient from 15 to 100% MeCN (18 min), isocratic 100% MeCN (4 min) at a flow rate of 1 mL.min⁻¹, UV detection at 330 nm. High resolution mass spectrometry measurements were performed at Centre Commun de Spectrometrie de Masse (Villeurbanne, France)

2. To a solution of methyl 6-(hydroxymethyl)-4-iodopicolinate (1.56 g, 5.33x10⁻³ mol, 1.0 eq) in distilled THF (50 mL) was added triethylamine (1.63 mg, 16x10⁻³ mol, 3.0 eq) and mesyl chloride (976 mg, 8.53x10⁻³ mol, 1.6eq). Reaction mixture was stirred under nitrogen atmosphere at room temperature for 4h. Then the solvent was evaporated under reduce pressure, the crude residue was dissolved in ethyl acetate and the solution was washed with a saturated aqueous NaHCO₃ solution, then with water. The organic layer was dried over Na₂SO₄ and the solvent removed at reduce pressure. The crude product was purified by flash chromatography (CH₂Cl₂/ MeOH from 0 to 5%) to give the desired product as a white solid (1.40g, 71%). ¹H NMR (500 MHz, CDCl₃) δ: 8.47 (d, ⁴J=1.5 Hz, 1H), 8.05 (d, ⁴J=1.5 Hz, 1H), 5.37 (s, 2H), 4.00 (s, 3H), 3.16 (s, 3H). ¹³C NMR (125 MHz, CDCl₃) δ: 164.1, 155.2, 148.0, 134.4, 134.3, 107.3, 70.0, 53.5, 38.3. HRMS (ESI⁺): (Calc for C₉H₁₀NO₅S: 370.93); [MH]⁺: m/z= 393.9217

3. To a suspension of Na₂CO₃ (1.59 g, 15x10⁻³ mol, 10eq) in acetonitrile (60 mL) were added under argon atmosphere TACN.3HCl (356 mg, 1.5x10⁻³ mol, 1.0 eq) and compound **2** (1.4 g, 4.79x10⁻³ mol, 3.2 eq). The reaction mixture was stirred at 60°C for 48 hours. The mixture was then cooled down and filtered. The filtrate was concentrated to dryness and the residue was purified by precipitation from ethyl acetate to give the desired product as a white solid (814 mg, 57%). ¹H NMR (200 MHz, CDCl₃) δ: 8.35 (d, J=1.4 Hz, 3H), 8.21 (d, J=1.4 Hz, 3H), 3.97 (s, 9H), 3.93 (s, 6H), 2.90 (s, 12H). ¹³C NMR (75 MHz, CDCl₃) δ: 164.6, 161.9, 147.6, 147.6, 135.6, 132.8, 106.6, 64.0, 56.1, 53.2. HRMS (ESI⁺): (Calc for C₃₀H₃₃I₃N₆O₆: 954.9627); [MH]⁺: m/z= 954.9668.

4. In a Schlenk tube were introduced compound **3** (150 mg, 1.57x10⁻⁴ mol, 1.0 eq) and 4-methoxyphenylboronic acid (79 mg, 5.18x10⁻⁴ mol, 3.3 eq) to a solution of anhydrous DMF (4 mL). The mixture was degassed under argon during 30 min. Then, Cs₂CO₃ (215 mg, 6.59x10⁻⁴ mol, 4.2 eq) and Pd(PPh₃)₄ (10 mg, 9.42x10⁻⁶ mol, 0.06 eq) were added. The reaction mixture was stirred under argon atmosphere during 48h at 100°C. The mixture was cooled down and Cs₂CO₃ filtered. The filtrate was concentrated to dryness and the residue was dissolved in CH₂Cl₂. The solution was washed with a saturated aqueous NaCl

PREPRINT

solution, then with water. The organic layer was dried over Na₂SO₄ and the solvent removed under reduced pressure. The crude product was purified by several washings in CH₂Cl₂/Et₂O mixtures and precipitation with pentane and isolated as a pale yellow solid (58 mg, 41%). ¹H NMR (200 MHz, CDCl₃) δ: 8.19 (s, 3H), 8.02 (s, 3H), 7.58 (d, 6H, *J* = 8.8 Hz), 6.94 (d, 6H, *J* = 8.9 Hz), 4.02 (s, 6H), 3.99 (s, 9H), 3.85 (s, 9H), 3.02 (brs, 12H). ¹³C NMR (50.32 MHz, CDCl₃) δ: 166.3, 161.8, 161.0, 149.4, 147.9, 129.6, 128.3, 123.3, 121.2, 114.8, 65.0, 56.5, 55.6, 29.9. HRMS (ESI⁺): (Calc for C₅₁H₅₅N₆O₉: 895.4032); [MH]⁺: *m/z* = 895.4025.

[TbL²]. To a solution of **4** (35 mg, 3.91 × 10⁻⁵ mol, 1.0 eq) in MeOH (10 mL) was added 10 mL of an aqueous solution of NaOH (1M). The reaction mixture was stirred at room temperature for 1 h. An aqueous solution of HCl (1M) was then added to the reaction mixture until pH = 2. K₂CO₃ (3.3 eq) and TbCl₃·6H₂O (44 mg, 1.17 × 10⁻⁴ mol, 3.0 eq) were added to the solution and the mixture was stirred at 50 °C for 16 h. The solution was cooled down and the solution evaporated to dryness. The crude product was purified by several triturations and precipitations from water. The purity of the complex was established by HPLC analysis (RT = 9.17 min). HRMS (ESI⁺): (Calc for C₄₈H₄₅N₆Na₂O₉Tb: 527.1144); [M+2Na]²⁺: *m/z* = 527.1143.

Cell culturing and treatment. We used T24 human epithelial bladder cancer cell line (ATCC No HBT-4). In our experiments, T24 cells were cultured in 25 cm² tissue-culture flasks (T25) at 37 °C, in a humidified atmosphere with 5% CO₂. They were incubated in RPMI 1640 supplemented with 100 U/mL penicillin, 100 μg/mL streptomycin, and 10% fetal calf serum (complete medium). Cells were grown to near confluence in the culture flasks and then suspended with 0.05% trypsin–EDTA solution (Sigma).

Twenty-four hours before experiments, cells were placed on LabTek I chambered cover glass (Nunc) at low cell density in complete culture medium. After being washed with the phosphate buffer saline (PBS), cells were fixed using paraformaldehyde (PFA 3% in PBS) for 10 min, permeabilized with PBS containing 0.5% Triton X100 for 10 min, and then washed again with PBS.

Microscopy. All confocal experiments were performed using a LSM710 NLO (Carl Zeiss) confocal laser scanning microscope based on the inverted motorized stand (AxioObserver). The excitation was selected by the acousto-optical modulator and provided by either 405 nm DPSS cw laser or Ti:Sa femtosecond tunable laser (Chameleon, Ultra II, Coherent) for 2P excitation in descanned detection mode. In the former case the pinhole was closed to 1 Airy Unit and in the latter one it was fully open. Multiplexed imaging was realized using a spectral detection mode of LSM710 in the range 422–655 nm with the resolution of 9.7 nm and a subsequent spectral unmixing with the reference spectra of each compound.

Acknowledgement. Authors thank Lyon Science Transfer agency for financial support and for a grant to V.P.

Notes and references

^a Laboratoire de Chimie UMR UMR 5182 CNRS-University Lyon- ENS Lyon, 46 allée d'Italie 69364 Lyon, France. olivier.maury@ens-lyon.fr

^b INSERM, IAB, F-38000, Grenoble, France

^c Univ. Grenoble Alpes, IAB, F-38000, Grenoble, France.

1 For reviews see : a) C. Andraud and O. Maury, *Eur. J. Inorg. Chem.* 2009, 4357 ; b) Y. Ma and Y. Wang, *Coord. Chem. Rev.*, 2010, **254**, 972-990.

2 a) G. S. He, L.-S. Tan, Q. Zheng and P. N. Prasad, *Chem. Rev.*, 2008, **108**, 1245-1330; b) M. Pawlicki, H. A. Collins, R. G. Denning and H. L. Anderson, *Angew. Chem. Int. Ed.* 2009, **48**, 3244 – 3266; c) A. V. Sarkar, D. E. Kang and B. R. Cho *Inorg. Chem.*, 2014, **53**, 1794-1803. For selected examples see: d) X. Zhang, Y. Xiao, J. Qi, J. Qu, B. Kim, X. Yue, K. D. Belfield *J. Org. Chem.* 2013, **78**, 9153–9160; e) L. Zhou, X. Zhang, Q. Wang, Y. Lv, G. Mao, A. Luo, Y. Wu, Y. Wu, J. Zhang, W. Tan, *J. Am. Chem. Soc.* 2014, **136**, 9838–9841 ; f) J. Massin, A. Charaf-Eddin, F. Appaix, Y. Bretonniere, D. Jacquemin, B. van der Sanden, C. Monnereau, C. Andraud, *Chem. Sci.* **2013**, **4**, 2833.

3 a) J.-C. Bünzli and S. Eliseeva, in *Lanthanide Luminescence*, eds. P. Hänninen and H. Härmä, Springer Berlin Heidelberg, 2011, vol. 7, ch. 3, pp. 1-45; b) J.-C. G. Bünzli, *Chem. Rev.*, 2010, **110**, 2729-2755; c) C. P. Montgomery, B. S. Murray, E. J. New, R. Pal and D. Parker, *Acc. Chem. Res.* 2009, **42**, 925; d) E. G. Moore, A. P. S. Samuel and K. N. Raymond, *Acc. Chem. Res.* 2009, **42**, 542; e) E. J. New, D. Parker, D. G. Smith and J. W. Walton *Curr. Opin. Chem. Biol.* 2010, **14**, 238–246; f) A. D'Aléo, L. Ouahab, C. Andraud, F. Pointillart, M. O., *Coord. Chem Rev.* 2012, **256**, 1604-1620; g) J. M. Zwier, H. Bazin, L. Lamarque and G. Mathis, *Inorg. Chem.*, 2014, **53**, 1854-1866; h) M. Rajendran, E. Yapici, and L. W. Miller *Inorg. Chem.*, 2014, **53**, 1839-1853; h) D. Geißler, S. Linden, K. Liermann, K. D. Wegner, L. J. Charbonnière, N Hildebrandt *Inorg. Chem.*, 2014, **53**, 1824-1838.

4 a) G. Piszczek, I. Gryczynski, B. P. Maliwal and L. J. R., *J. Fluoresc.* 2002, **12**, 15; b) G. Piszczek, B. Maliwal, I. Gryczynski, J. Dattelbaum and J. Lakowicz, *J. Fluoresc.*, 2001, **11**, 101-107; c) M. H. V. Werts, N. Nerambourg, D. Pelegru, Y. L. Grand and M. Blanchard-Desce, *Photochem. Photobiol. Sci.*, 2005, **4**, 531-538; d) L.-M. Fu, X.-F. Wen, X.-C. Ai, Y. Sun, Y.-S. Wu, J.-P. Zhang and Y. Wang, *Angew. Chem., Int. Ed.*, 2005, **44**, 747-750; e) A. D'Aléo, A. Picot, P. L. Baldeck, C. Andraud and O. Maury, *Inorg. Chem.*, 2008, **47**, 10269-10279.

5 a) A. Picot, A. D'Aléo, P. L. Baldeck, A. Grichine, A. Duperray, C. Andraud, O. Maury, *J. Am. Chem. Soc.* 2008, **130**, 1532; b) G.-L. Law, K.-L. Wong, C. W.-Y. Man, W.-T. Wong, S.-W. Tsao, M. H.-W. Lam, P. K.-S. Lam, *J. Am. Chem. Soc.* 2008, **130**, 3714; c) F. Kielar, A. Congreve, G.-I. Law, E. J. New, D. Parker, K.-L. Wong, P. Castreno, J. de Mendoza, *Chem. Commun.* 2008, 2435.

- 6 a) S. V. Eliseeva, G. Auböck, F. van Mourik, A. Cannizzo, B. Song, E. Deiters, A.-S. Chauvin, M. Chergui and J.-C. G. Bünzli, *J. Phys. Chem. B*, 2010, **114**, 2932-293; b) G. Shao, R. Han, Y. Ma, M. Tang, F. Xue, Y. Sha, Y. Wang, *Chem. Eur. J.* 2010, **16**, 8647-8651; c) Z.-J. Hu, X.-H. Tian, X.-H. Zhao, P. Wang, Q. Zhang, P.-P. Sun, J.-Y. Wu, J.-X. Yang and Y.-P. Tian, *Chem. Commun.*, 2011, **47**, 12467-12469; d) W.-S. Lo, W.-M. Kwok, G.-L. Law, C.-T. Yeung, C. T.-L. Chan, H.-L. Yeung, H.-K. Kong, C.-H. Chen, M. B. Murphy, K.-L. Wong and W.-T. Wong, *Inorg. Chem.*, 2011, **50**, 5309-5311; e) E. Baggaley, D.-K. Cao, D. Sykes, S. W. Botchway, J. A. Weinstein and M. D. Ward, *Chem. Eur. J.*, 2014, **20**, 8898-8903
- 7 a) T. Zhang, X. Zhu, C. C. W. Cheng, W.-M. Kwok, H.-L. Tam, J. Hao, D. W. J. Kwong, W.-K. Wong and K.-L. Wong, *J. Am. Chem. Soc.*, 2011, **133**, 20120-20122; b) T. Zhang, X. Zhu, W.-K. Wong, H.-L. Tam and W.-Y. Wong, *Chem. Eur. J.*, 2013, **19**, 739-748; c) A. Bourdolle, M. Allali, A. D'Aléo, P. L. Baldeck, K. Kamada, J. A. G. Williams, H. Le Bozec, C. Andraud and O. Maury *ChemPhysChem* 2013, **14**, 3361-3367.
- 8 D'Aléo, A. Bourdolle, S. Brustlein, T. Fauquier, A. Grichine, A. Duperray, P. L. Baldeck, C. Andraud, S. Brasselet and O. Maury, *Angew. Chem., Int. Ed.*, 2012, **51**, 6622-6625
- 9 a) C. Philippot, A. Bourdolle, O. Maury, F. Dubois, B. Boury, S. Brustlein, S. Brasselet, C. Andraud and A. Ibanez, *J. Mat. Chem.*, 2011, **21**, 18613-18622; b) G. Lapadula, A. Bourdolle, F. Allouche, M. Conley, I. del Rosa, L. Maron, W. W. Lukens, Y. Guyot, C. Andraud, S. Brasselet, C. Copéret, O. Maury and R. A. Andersen. *Chem. Mater.* 2014, **26**, 1062-1073.
- 10 A. Grichine, A. Haefele, S. Pascal, A. Duperray, R. Michel, C. Andraud and O. Maury *Chem. Science*, 2014, **5**, 3475-3485.
- 11 H. H. Gorris and O. S. Wolbeis, *Angew. Chem. Int. Ed.* 2013, **52**, 3584-3600; b) V. Fernandez-Moreira, B. Song, V. Sivagnanam, A.-S. Chauvin, C. D. B. Vandevyver, M. A. M. Gijs, I. A. Hemmilä, H.-A. Lehrand, J.-C. G. Bünzli *Analyst*, **2010**, *135*, 42-52
- 12 a) J. W. Walton, A. Bourdolle, S. J. Butler, M. Soulie, M. Delbianco, B. K. McMahon, R. Pal, H. Puschmann, J. M. Zwier, L. Lamarque, O. Maury, C. Andraud and D. Parker, *Chem. Commun.*, 2013, **49**, 1600-1602; b) M. Soulie, F. Latzko, E. Bourrier, V. Placide, S. J. Butler, R. Pal, J. W. Walton, P. L. Baldeck, B. Le Guennic, C. Andraud, J. M. Zwier, L. Lamarque, D. Parker and O. Maury *Chem. Eur. J.* 2014, **20**, 8636 - 8646; c) S. J. Butler, L. Lamarque, Robert Pal, D. Parker *Chem. Sci.*, 2014, **5**, 1750-1756.
- 13 V. Placide, D. Pitrat, A. Grichine, A. Duperray, C. Andraud and O. Maury *Tetrahedron Lett.*, 2014, **55**, 1357-1361.
- 14 V. Placide, D. Pitrat, C. Andraud and O. Maury Priority Application Number FR2013-053037.
- 15 G. Nocton, A. Nonat, C. Gateau, M. Mazzanti, *Helv. Chem. Acta* 2009, **92**, 2257.
- 16 A. Bourdolle, M. Allali, J.-C. Mulatier, B. Le Guennic, J. M. Zwier, P. L. Baldeck, J.-C. G. Bünzli, C. Andraud, L. Lamarque, O. Maury, *Inorg. Chem.* 2011, **50**, 4987